CrystEngComm

Accepted Manuscript

ROYAL SOCIETY OF CHEMISTRY

www.rsc.org/crystengcomm

A new 3D four-fold interpenetrated dia-like polymer: gas sorption and computational analyses

Jian Wu[a], Jian-Qiang Liu[b*], Zhen-Bin Jia[b], Qing-Lin Li[b], Kai-Bang Li[a], Hao Li[a], Carole Daiguebonne[c], Guillaume Calvez[c], Olivier Guillou[c*]

[a] *Guangxi Key Laboratory of Chemistry and Engineering of Forest Products, Guangxi University for Nationalities, College of Chemistry and Chemical Engineering, Nanning, Guangxi 530006, China*
[b] *School of Pharmacy, Guangdong Medical College, Dongguan 523808, China*
[c] *INSA, UMR 6226 "Institut des Sciences Chimiques de Rennes", F-35708 Rennes, France*
Corresponding author: jianqiangliu2010@126.com (J.-Q. Liu) and Olivier.Guillou@insa-rennes.fr(O. Guillou).

Abstract:

A new metal-organic framework, namely, $\{[Cu(bib)_2]\cdot NO_3\cdot 4H_2O\}_n$ (**1**) (bib = 2,3-bis(4-pyridyl)butane), was synthesized and characterized. In the structure of **1**, nitrogen atoms of four bib ligands bind to the tetrahedrally coordinated metal ion. The bib ligands act as linear bidenate linkers to form a four-fold interpenetrated 3D framework with a **dia**-like topology. The H_2 uptake of the dehydrated coordination framework **1** was estimated using a computational method based on Connolly's algorithm, indicating that adsorbed H_2 is predominantly located around the outer surface of the pore through multipoint interactions with the inner surface of dehydrated **1'**. The material has no significant adsorption for CO_2 and N_2 gas upon desolvation by long-time thermal activation, indicating that access to the void space is blocked by the large and immovable anions. The luminescent properties of sample **1** and dehydrated sample **1'** were also explored.

Keywords: Gas sorption; interpenetration; luminescence

Introduction

Materials called metal−organic frameworks (MOFs), a term introduced in the early 1990's by Robson, Yaghi, Zaworotko and James, describes a class of porous polymeric materials that consist of metal ions linked together by organic bridging ligands [1]. The porous yet rigid nature of these coordination networks has since then attracted substantial attention, mainly because of their potential to sustain permanent porosity with specific surface areas surpassing even those of the well-known zeolites and porous silicates. Their

extraordinarily low densities and high surface areas make these materials extremely useful in a wide range of applications that range from adsorption, storage and separation of gases such as hydrogen or methane, over capture of carbon dioxide, to heterogeneous catalysis, to name just a few [1]. Thanks to the large variety of metal centers, commonly called nodes, and of organic bridging ligands, referred to as linkers, there is a virtually limitless possibility of combination of secondary building units that can be assembled interesting MOFs. This extreme diversity does also pose challenges, both for categorizing the different classes of MOFs, and for predicting which molecular architecture – or topology might form with a selection of nodes and linkers under reaction conditions [2-6]. Both of these problems have led to the establishment of a complete new subject in solid state sciences now commonly called "Reticular Chemistry", which tries to describe and explain the design of solid materials from molecular building blocks.

One gateway towards the formation of highly porous MOF like materials is the use of long extended linkers. A side effect of this strategy is the possibility to also form interpenetrating networks, *i.e*. structures with entangled frameworks not connected through any covalent interactions. This subcategory of MOFs encompasses a variety of interesting topological species such as *e.g*. polyknot and polycatenation compounds. The formation of entangled coordination polymers is additionally promoted by the use of not only elongated but also flexible organic linkers. For example, the flexible organic linker 1,2–bis(4-pyridyl)ethane is an excellent building block to construct different MOFs with well properties[7-11]. Thus, one effective way to modulate the type of entangled topological motif is to vary the flexibility and length of the ligand. We have been interested in the syntheses and characterization of entangled MOFs containing the extended organic linker 2,3-bis(4-pyridyl)butane, which so far has led to the formation of 2D→2D parallel interpenetrated frameworks with polyrotaxane and polycatenane character [12].

The two main factors which affect the adsorption of gases in a microporous solid are: (a) the affinity of the surface for the adsorbates, and (b) the confinement effects generated within the cavities from the overlap of the potential energy surfaces of the guest molecules with the atoms of the host framework. The former factor can be directed through the functionalization of the MOFs, which has been investigated vigorously [13].

The functionalization method utilizes e.g. linkers containing halogen atoms, amine, amide, or alkyl groups. Postsynthetic modifications have also been described. However, the above method is confined by chemical incompatibilities of functional groups with the MOF assembly, and also by the rigidity of the MOF itself. Recently, a few of MOFs were prepared with using of flexible linkers [14-15]. Extending our previous work on the self-assembly of novel topological coordination polymers based on the conformationally flexible bib ligand, herein, we report the compound $\{[Cu(bib)_2]\cdot NO_3\cdot 4H_2O\}_n$ (**1**) (bib = 2,3-bis(4-pyridyl)butane), which shows 4-fold interpenetrated 3D framework with a **dia**-like topology. Furthermore, its gas adsorption and luminescence properties are discussed in detail.

Experimental

Materials and Method

All reagents were purchased from commercial sources and used as received. IR spectra were recorded with a Perkin–Elmer Spectrum One spectrometer in the region 4000–400cm^{-1} using KBr pellets. TGA were carried out with a Metter–Toledo TA 50 in dry dinitrogen (60mL.min^{-1}) at a heating rate of 5°C min^{-1}. X-ray powder diffraction (XRPD) data were recorded on a Rigaku RU200 diffractometer at 60KV, 300mA with *Cu* K_α radiation (λ = 1.5406 Å), with a scan speed of 2 °C/min and a step size of 0.013° in 2θ. Luminescence spectra for crystal solid samples were recorded at room temperature on an Edinburgh FLS920 phosphorimeter (USA). All the gas sorption isotherms were measured by using a ASAP 2020M adsorption equipment.

X-ray Crystallography

Single crystal X-ray diffraction analysis of the compound was carried out on a *Bruker SMART APEX II CCD* diffractometer equipped with graphite monochromated Mo*K*α radiation (λ = 0.71073 Å) by using ϕ/ω scan technique at room temperature. The intensities were corrected for Lorentz and polarization effects as well as for empirical absorption based on multi-scan techniques; the structures was solved by direct methods and refined by full-matrix least-squares fitting on F^2 using SHEXL-97[16]. Absorption corrections were applied using the multi-scan approach with the program SADABS [17]. Indeed, the unit cell volume includes a large region of disordered nitrate and water molecules which could not be modeled as well discrete atomic sites, but their

compositions can be confirmed by XPS, elemental analysis data, IR and TGA. Thus, they are included in the final formula. The formulation is supported by other chemical analyses. The crystal structure analysis, however, is unambiguous in the context of connectivity. The core fragment of the ligand, consisting of the two C-H and two methyl groups, is disordered over two alternative orientations. The disordered atoms were subjected to a rigid bond restraint. Subject to these conditions the occupancies refined to 0.67(4) and 0.33(4). The nitrate ion located within the void space of the metal-ligand framework is highly disordered and/or incompatible with the tetragonal symmetry. It was added to the structural model using a rigid model and disordered over four symmetry equivalent sites with each one quarter occupancy, and it was refined as disordered with four water molecules. Table 1 shows crystallographic data of **1**. Selected bond distances and bond angles are listed in Table 2. **CCDC**: 972847.

Synthesis of complex 1

A mixture of $Cu(NO_3)_2$ (0.1 mmol), bib (0.1 mmol), CH_3OH (2 mL) and deionised water (10 mL) was placed in a Teflonlined stainless steel vessel, heated to 160 °C for 3 days under autogenous pressure, and then cooled to room temperature at a rate of 5 °C/h. Yellow crystals were obtained. The resulting crystals formed were filtered off, washed with water and dried in air. $C_{28}H_{40}CuN_5O_7$ (622.19). Calcd: C, 54.05; H, 6.48; N, 11.26. Found C, 55.33; H, 6.20; N, 11.41. **IR** (KBr, cm^{-1}): 3426(vs); 3118(m); 2219(m); 1620(m); 1492(s);1344(s);1259(vs); 730(vs). Raman: 1012(m); 1219(w); 1609(vs).

Results and Discussion

Compound **1** was synthesized in a solvent system composed of methanol (CH_3OH). The **1** cannot be obtained under low temperature, the reaction used of the same reactant process employed for the synthesis of **1** under 120 °C, which led to the formation of powder. Moreover, the pH value of the reaction solution does not play a role key in determining the final products, although we have tried to adjust the pH (such as 6 and 7.5) at different degrees. During the reaction process, the Cu(II) ions were reduced in situ to form Cu(I). The XPS spectrum results (932.8 eV Cu(I) character) indicate that Cu(I) is present in the coordination polymer of **1** (Fig. S1). Compound **1** crystallizes in the tetragonal crystal system with the space group *P*4/*n*. In the asymmetric unit there are one crystallographically independent Cu(I) centre, two bib linkers, one nitrate anion and four

water molecules. The Cu1 atom lies on the four fold axis (Fig. 1).The charge of the cationic framework is balanced by the guest nitrate anions. In **1**, each Cu(I) ion is coordinated by four nitrogen atoms from four independent bib ligands (Fig. 1), in other words, the bib linkers connect Cu(I) centers in four directions, generating a 3-D porous MOF along the c axis (Fig. 2a). The Cu(I) centers serve as 4-connected tetrahedral nodes to result in a **dia** topology with a point symbol of ($6_2.6_2.6_2.6_2.6_2.6_2$) (Fig. 2b) [18]. The spaciousness of the net leads to the interpenetration of four identical nets (Fig. 2c). Compound **1** exhibits a four-fold parallel interpenetrating array to minimize the big void space and stabilize the framework. Viewed along the *a* axis, there are grid channels with a diameter of 10.1×8.9 Å. The effective free volume of **1**, calculated by PLATON analysis, is 6.2 % (1778.3 $Å^3$ per unit) without consideration of the water molecules [19]. Polymer **1** has an usual 4-fold interpenetrated 3-D architecture with helical channels (Fig. 3). To the best of our knowledge, complex **1** is the first representative of this kind of 4-fold interpenetrated framework with only bib ligand (Fig.4).

IR, **Thermogravimetric Analyses and XRPD**

As to FTIR spectra (Fig. S2), the compound shows a broad band centered around 3482 cm^{-1} may be attributed to the O-H stretching frequency of the water molecules in **1**. The O–H stretching vibration for *Ic* appears as a broad band centered around 3500 cm^{-1} [20]. The peak at around 1620 cm^{-1} is assigned to the $\upsilon(NO_3^-)$ asymmetric and symmetric stretching vibrations in **1**.

To study the stability of the coordination polymer, thermogravimetric analysis (TGA) of complex **1** was performed (Fig. S3). Compound **1** shows three of weight loss steps. The first weight loss begins at 20 °C and is completed at 115 °C. The observed weight loss of 12.3 % is corresponding to the loss of the four crystallization water molecules (calcd 11.6 %). The second weight loss occurs in the range 140−429 °C, which can be attributed to the elimination of one bib organic ligand. Removal of all organic components was completely by 429 °C, indicated by a further weight loss of 78.77% (calcd 78.13 %), roughly consistent with expulsion of the bib and the nitrate molecules.

To confirm the phase purity of the compound, the original sample was characterized by X-ray powder diffraction (XRPD) at room temperature. The pattern that simulated from the single-crystal X-ray data of compound was in agreement with the observed

experimental pattern, as shown in Fig. S4. Heating of **1** to 120 °C for 4 h removes the free water to form the "evacuated" framework is defined as **1'**. The XRPD pattern of **1'** is not similar to that of compound **1**. Moreover, the pale yellow color of sample **1** changed in the process to a greenish-gray color of sample **1'**, and crystals of **1'** become brittle and can easily be broken. We tried to collect the single crystal XRD data of **1'**, however, the sample **1'** diffracts much weaker than that original sample **1** and no usable SC XPD data could be obtained. We attribute this feature of sample **1'** to a stabilizing effect of the guest water molecules through strong hydrogen bonding interactions with the nitrate anion. Loss of the water molecules also can be expected to lead to a more flexible and less rigid nature for the remaining structure, thus leading to weaker overall diffraction.

Organic–inorganic coordination polymers, especially those with d^{10} metal centers, have been investigated for their fluorescent properties and potential applications as fluorescen-emitting materials, such as light-emitting diodes (LEDs) [21]. Therefore, the complex **1** was studied in the solid-state at room temperature (Fig. 5). Excitation of the microcrystalline sample at 346 nm leads to the generation of fluorescent emission, with the peak maxima occurring at 585 nm for **1**. The spectrum of **1'** is similar to that of complex **1**, but the intensity is weaker and the main peak of **1'** is blue-shifted by about 28 nm compared to compound **1**. The above luminescent phenomenon is presumably due to the more rigid nature architecture of **1**, when compared to dehydrated **1'**. In the original crystal, abundant lattice water molecules fill in the network and interact through weak forces such as hydrogen bonds with the framework lattice of **1**. These weak forces do not only stabilize the framework and enhance its rigid structure, but they also affect the transfer of energy effectively from the bib to the metal center. Accordingly, some guest molecules are removed from **1**, in which undoubtedly decreasing the weak interactions. Therefore, the emission spectrum becomes weaker, and the main peak is shifted. Moreover, this compound exhibits strong photoluminescence at room temperature and may be suitable as a candidate of luminescent materials [22].

The fluorescence lifetime τ values of **1** and **1'** are on the nanosecond timescale at room temperature, as shown in Fig.S3. The χ^2 values are found to be close to 1.0 in both compounds. Interestingly, the complexes **1** and **1'** have lifetimes in the range 4.2 ns for **1** and 2.8 ns for **1'**at the same excitation wavelength (λ_{em} = 346 nm), respectively, as shown

in Fig. S5.

Gas sorption properties

From Fig. 6, it can be observed that the amount of CO_2 sorption rises gradually from P/P_0 = 0 to 1.0. This is a Type I isotherm behavior typical for the microporous materials but similar to Type II or Type III isotherms as defined by the IUPAC classification [23]. This unusual sorption feature can be attributed to one of two reasons: on the one hand, **1** is a cation framework and its channels may be blocked by the large and immovable nitrate anions; on the other hand, the interaction between CO_2 molecules and the cation framework is very weak. Comparison of the CO_2 sorption curve with the N_2 curve indicates that the latter reason can exclude as the main cause of the weak adsorption of CO_2 into the framework of **1**. The high N_2 gas sorption amount shows 29 cm^3(STP)/g at $P/P0$ = 1.0 and 77 K, and exhibits no significant hysteresis between sorption and desorption traces, indicating **1** to not be a microporous material [24].

To understand the solvent dependence of gas adsorption behavior in this MOF, grand canonical Monte Carlo (GCMC) simulations using standard algorithms were performed to predict H_2 adsorption isotherms. The simulation cell consists of 2×2×1 unit cells of the MOF. Periodic boundary conditions were applied in all three dimensions. For each state point, the GCMC simulation consisted of 1×10^7 steps to guarantee equilibration followed by 1×10^7 steps to sample the desired thermodynamic properties. H_2 and MOF interactions are modeled by Lennard-Jones potential between all pairs of sites. GCMC simulations were performed at 77 K [25], in the pressure range p =0–1000.0 KPa. From Figure 7 we can see that H_2 uptake in this MOF containing solvent molecules is 10mmol/g at 77K with 1000 kPa, but it is 45 mmol/g H_2 adsorption in MOF without solvent molecules.

In order to understand the reason that H_2 adsorption of MOF containing solvent molecules is lower than MOF without solvent molecules, we calculate the Connolly Surfaces of MOF containing solvents and MOF without solvents, respectively. The calculated results show that this MOF surface area is reduced significantly by solvent molecules from 734.83 $Å^2$ to 189.72 $Å^2$. This conclusion can be confirmed by a molecular calculation (See Table S1 and Fig. S6). This could suggest that upon de-hydration, the molecular framework collapses. The XRD and TGA diagrams confirm this hypothesis (Fig. S3 and Fig. S4). The decomposition of sample **1'** starts over at 150 º.

Thus, the sample **1'** shows little gas sorption at low pressure.

The bonding sites of H_2 with MOF are given in Figure 8. From Figure 8(a), it can be seen that the first H_2 molecule is located at the centre of solvent molecules, and average distance between H atom and O atom is 2.583 Å. The interaction between H_2 and MOF is mainly van der waals energy about -0.318kcal/mol. As comparison, Figure 8(b) show that the first H_2 molecule is absorbed by-CH_3 group of ligand, the nearest distance between H atom and C atom is 2.854 Å. van der waals interaction (-0.204 kcal/mol) also is mainly interaction between H_2 and MOF. The snapshot of the MOF with H_2 at 1000 kPa pressures is shown in Figure 9. For framework containing solvent molecules, the negative potential locates around solvent molecules and major H_2 close to solvents. But for framework without solvent molecules, the negative potential spreads along edge of pores and partial H_2 molecules are absorbed around ligands. Please note, metal Cu scarcely absorbs any H_2 whether MOF containing solvents or without solvents. In conclusion, the solvent molecules in MOF reduce the surface area and negative potential ranges, leading to a smaller gas absorbed amounts [26].

Conclusions

In summary, we have successfully synthesized a new 3D porous cation framework constructed from a flexible N-donor ligand. It shows a four-fold interpenetrated 3D framework with a **dia**-like topology. The compound exhibits strong photoluminescence at room temperature and may be suitable as a candidate as a luminescent materials. The H_2 adsorption isotherm of the dehydrated coordination framework of **1'** was estimated by Connolly's algorithm. We hope that the synthetic methods described herein will further facilitate the exploration of new types of multifunctional materials with interesting properties, including the combination of porosity and luminescence.

Acknowledgments

This work was partially supported by the Grants from the National Natural Science Foundation of China (21201044), Natural Science Foundation of Guangdong Province (S2012040007835), Foundation for Distinguished Young Talents in Higher Education of Guangdong Province (LYM11069), Guangxi University for Nationalities (2011DQ022), Training plan of Guangdong Province outstanding young teachers in Higher Education Institutions (Grant No.YQ2013084), and thanks to Dr. C. H. Zhou, and Matt Zeller for discussion.

References:

1 (a) M. Eddaoudi, D. B. Moler, H. Li, B. Chen, T. M. Reineke, M. O'Keeffe and O. M. Yaghi, *Acc. Chem. Res*., 2001, **34**, 319; (b) S. James, *Chem. Soc. Rev.***,** 2003, **32**, 276; (c) S. R. Batten and R. Robson, *Angew. Chem., Int. Ed*., 1998, **37**,1460; (d) N. W. Ockwig, O. D-Friedrichs, M. O'Keeffe and O. M. Yaghi, *Acc.Chem. Res*., 2005, **38**, 176; (e) B.Moulton and M. J. Zaworotko. *Chem. Rev*., 2001 , **101**, 1629.

2 (a) R. Martínez-Máñez and F. Sancenón, *Chem. Rev*., 2003, **103**, 4419; (b) J. P. Ma, Y. Yu and Y. B. Dong, *Chem. Commun*., 2012, **48**, 2946.

3 (a) B. F. Abrahams, S. R. Batten, H. Hamit, B. F. Hoskins and R. Robson, *Angew. Chem., Int. Ed. Engl.*, 1996, **35**, 1690; (c) V. A. Blatov, L. Carlucci, G. Ciani and D. M. Proserpio, *CrystEngComm*, 2004, **6**, 378; (d) Q. Lin, T. Wu, S. T. Zheng, X. H. Bu and P. Y. Feng, *J. Am. Chem. Soc*., 2012, **134**, 784.

4 (a) S. Kitagawa, R. Kitaura and S. Noro, *Angew. Chem., Int*. Ed., 2004, **43**, 2334; (b) J. R. Li,R. J.Kuppler and H. -C. Zhou, *Chem. Soc. Rev*., 2009, **38**, 1477; (c) J. Lee, O. K. Farha, J. Roberts, K. A. Scheidt, S. T. Nguyen and J. T. Hupp, *Chem. Soc. Rev*., 2009, **38**, 1450; (d) D. Maspoch, D. Ruiz-Molina and J. Veciana, *Chem. Soc. Rev*., 2007, **36**, 770.

5 (a) J.-P. Zhang, Y.-Y. Lin, X.-C. Huang and X.-M. *Chen, Cryst. Growth Des*., 2006, **6**, 519; (b) O. M. Yaghi and J. R. Long, *Chem. Soc. Rev*., 2009, **38**, 1203; (c) A. C. McKinlay, R. E. Morris, P. Horcajada, G. Férey, R. Gref, P. Couvreur and C. Serre, *Angew. Chem., Int. Ed*., 2010, **49**, 6260.

6 (a) S. R. Miller, E. Alvarez, L. Fradcourt, T. Devic, S. Wuttke, P. S. Wheatley, N. Steunou, C. Bonhomme, C. Gervais, D. Laurencin, R. E. Morris, A. Vimont, M. Daturi, P. Horcajada and C. Serre, *Chem. Commun*., 2013, **49**, 7773; (b) N. J. Hinks, A. C. McKinlay, B. Xiao, P. S. Wheatley and R. E. *Morris, Microporous Mesoporous Mater*., 2010, **129**, 330; (c) C. S. Allardyce, P. J. Dyson, D. J. Ellis and S. L. Heath, *Chem. Commun*., 2001, 1396.

7 (a) B. Chen, S. Xiang and G. Qian, *Acc. Chem. Res*., 2010, **43**, 1115; (b) J.-R. Li, J. Sculley and H.-C. Zhou, *Chem. Rev*., 2012, **112**, 869; (c) R.-Q. Zou, H. Sakurai, S. Han, R.-Q. Zhong and Q. Xu, *J. Am. Chem. Soc*., 2007, **129**, 8402; (d) C. Li, D.-S. Li, J. Zhao, Y.-Q. Mou, K. Zou, S.-Z. Xiao and M. Du, *CrystEngComm*, 2011, **13**, 6601; (e) C.-P. Li and M. Du, *Inorg. Chem. Commun.*, 2011, **14**, 502; (f) M. Du, C.-P. Li and J.-H. Guo, *CrystEngComm*, 2009, **11**, 1536.

8 (a) M. Du, C.-P. Li, J.-M. Wu, J.-H. Guo and G.-C. Wang, *Chem. Commun*., 2011, **47**, 8088; (b) X.-D. Zheng, L. Jiang, X.-L. Feng and T.-B. Lu, *Inorg. Chem*., 2008, **47**, 10858; (c) F.-N. Dai, H.-Y. He and D.-F. Sun, *Inorg. Chem*., 2009, **48**, 4613.

9 (a) X. H. Bu, M. L. Tong, H. C. Chang, S. Kitagawa and S. R. Batten, *Angew. Chem., Int. Ed*., 2004, **43**, 192; (b) G. P. Yang, L. Hou, X. J. Luan, B.Wu and Y. Y. Wang, *Chem. Soc. Rev*., 2012, **41**, 6992; (c) J. P. Zhang, X. L. Qi, C. T. He, Y. Wang and X. M. Chen, *Chem. Commun*., 2011, **47**, 4156.

10 (a) X. L.Wang, C. Qin, E. B.Wang, Y. G. Li, Z.M. Su, L. Xu and L. Carlucci, *Angew. Chem., Int. Ed*., 2005, **44**, 5824; (b) S. Kitagawa and R. Matsuda, *Coord. Chem. Rev*., 2007, **251**, 2490; (c) S. T. Hyde, M. O'Keeffe and D. M. Proserpio, *Angew. Chem., Int. Ed*., 2008, **47**, 7996; (d) E. V. Alexandrov, V. A. Blatov and D. M. Proserpio, *Acta Crystallogr., Sect. A*: Found. Crystallogr., 2012, **68**, 484; (e) H. Wu, J. Yang, Z. M. Su, S. R. Batten and J. F.Ma, *J. Am. Chem. Soc*., 2011, **133**, 11406; (f) M. Du, Z. H. Zhang, L. F. Tang, X. J. Zhao and S. R. Batten, *Chem.–Eur. J*., 2007, **13**, 2578.

11 (a) L. Carlucci, G. Ciani and D. M. Proserpio, *Coord. Chem. Rev*., 2003, **246**, 247; (b) X. L. Wang, C. Qin, E. B.Wang, Y. G. Li and Z.M. Su, *Chem. Commun*., 2005, 5450; (c) B. Xu, Z.He, Z. Lin and R. Cao, *Chem. Commun*., 2011, **47**, 3766; (d) L. Chen, Y. Q. Lan, S. L. Li, K. Z. Shao and Z. M. Su, *Chem. Commun*., 2012, **48**, 5919; (e) K. Zhou, F. L. Jiang, L. Chen,M. Y.Wu, S. Q. Zhang, J. Ma and M. C. Hong, *Chem. Commun*., 2012, **48,** 12168; (f) I. A. Baburin and S. Leoni, *CrystEngComm*, 2010, **12**, 2809; (g) H.Y. He, J.M. Dou, D. C. Li, H. Q. Ma and D. F. Sun, *CrystEngComm*., 2011, **13**, 1509; (h) B. Y. Li, G. H. Li, D. Liu, Y. Peng, X. J. Zhou, J. Hua, Z. Shi and S. H. Feng, *CrystEngComm*, 2011, **13**, 1291; (i) G. M. Sun, H. X. Huang, X. Z. Tian, Y. M. Song, Y. Zhu, Z. J. Yuan, W. Y. Xu, M. B. Luo, S. J. Liu, X. F. Feng and F. Luo. *CrystEngComm*, 2012, **14**, 6182.

12 J. Wu, J. Q. Liu, J. T. Lin, T. Wu, X. R. Wu, C. H. Zhou and X. Y. Qin, *Inorg. Chimi. Acta*., 2013, **405**, 65

13 D. A. Gomez, A. F. Combariza and G. Sastre, *Phys. Chem. Chem. Phys*., 2012, **14**, 2508.

14 C. Yang, X. Wang and M. A. Omary, *Angew. Chem., Int. Ed*., 2009, **48**, 2500.

15 S. K. Ghosh, S. Bureekaew and S. Kitagawa, *Angew. Chem., Int. Ed*., 2008, **47**, 3403.
16. G. M. Sheldrick, *SHELXL-97*: program for structure determination and Refinement.University of Göttingen: Göttingen, 1997.
17. G. M. Sheldrick, SADABS 2.05. University of Göttingen: Germany, 2002.
18 (a) O. V. Dolomanov, A. J. Blake, N. R. Charmpness and M. Schröder, *J. Appl. Crystallog*r. 2003, **24**, 776; (b) V. A. Blatov, M. O'Keeffe and D. M. Proserpio, *CrystEngComm*, 2010, **12**, 44.
19 A. L. Spek, *J. Appl. Crystallog*r. 2003, **36**, 7.
20 K. Nakamoto, *Infrared and Raman Spectra of Inorganic and Coordination Compounds*, 5th ed., Wiley Interscience, New York, 1997.
21 Y. Q. Chen, G. R. Li, Z. Chang, Y. K. Qu, Y. H. Zhang and X. H. Bu, *Chem. Sci*, 2013, **4**, 3678.
22 (a) L. Y. Zhang, J. P. hang, Y. Y. Lin and X. M. Chen, *Cryst. Growth. Des*., 2006, **6**, 1685; (b) Q. Chu, G. X. Lin, Huang, X. F. wang and W. Y. Sun, *Dalton Trans*., 2007, 4302; (c) Z. L. Chen, Y. Su, W. Xiong, L. X. Wang, Y. G. Li, N. Hao, C. W. Hu and L. Xu, *Inorg. Chem*., 2004, **43**, 1850.
23 F. Rouquerol, J. Rouquerol and K. Sing, *Adsorption by Powders and Porous Solids*, Academic Press, London, 1999.
24 G. C.Maitland, M. Rigby, E. B. Smith and W. A. Wakeham, *Intermolecular Forces*; Claredon Press: Oxford, U.K., 1981
25 (a) S. J. Grimme, *Comput. Chem*. 2006, **27**, 1787; (b) D. Frenkel and B. Smit, *Understanding Molecular Simulation*: *From Algorithms to Applications*; Academic Press: San Diego, CA, 2002.
26 P. Cui, Y. G. Ma, H. H. Li, B. Zhao, J. R. Li, P. Cheng, P. B. Balbuena and H. C. Zhou, *J. Am. Chem. Soc*., 2012, **134**, 18892.

Main Figures in the Text:

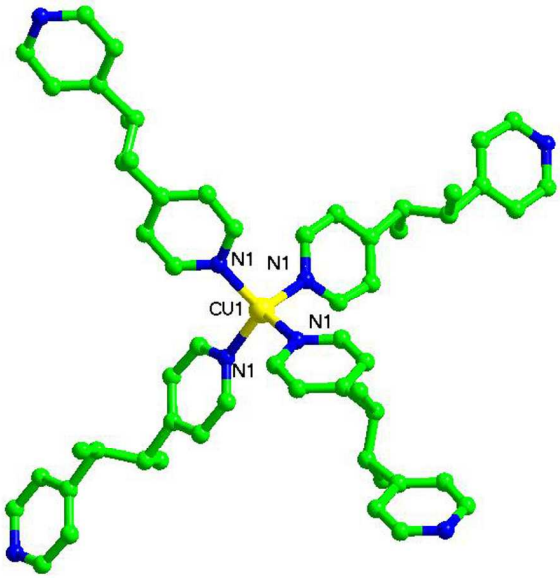

Fig.1 Asymmetric unit of **1** with thermal ellipsoids at 50% probability. The hydrogen atoms have been removed for clarity (symmetric code: y-1/2, -x+1, -z+1).

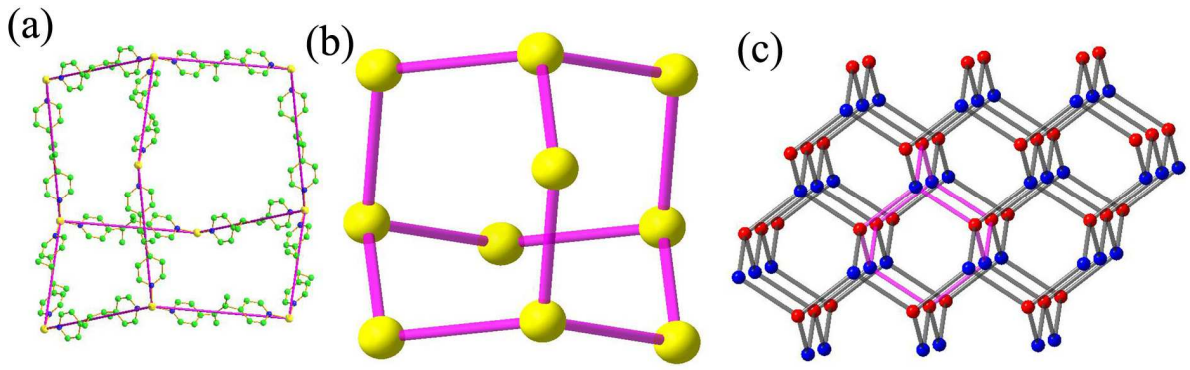

Fig.2 (a) view of the **dia**-like topology in **1**; (b) schematic present of **dia** network; and (c) the 3D network in **1**.

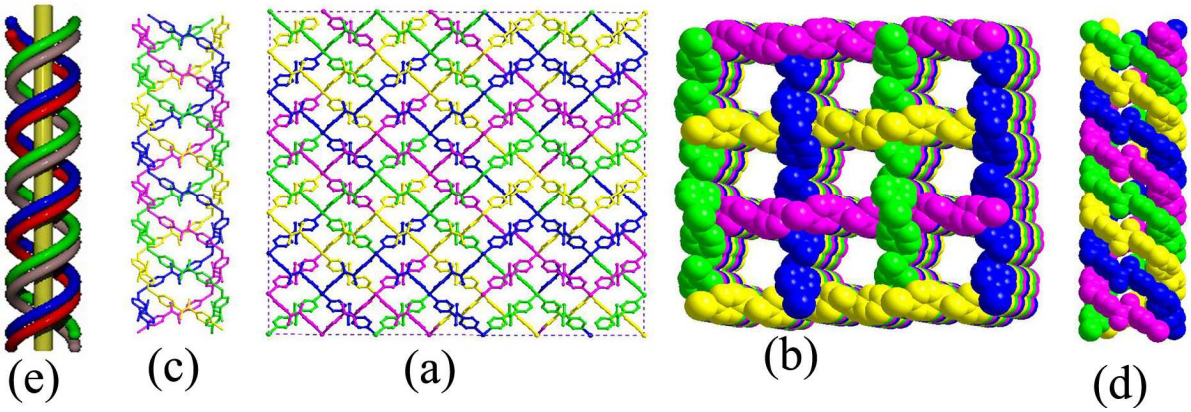

Fig. 3 (a) framework perspective of **1** showing the tetra-interpenetrating lattice; (b) view of the channel and helix chain; (c) and (d) the tetra-stranded helix; (e) schematic perspective of helix in **1**.

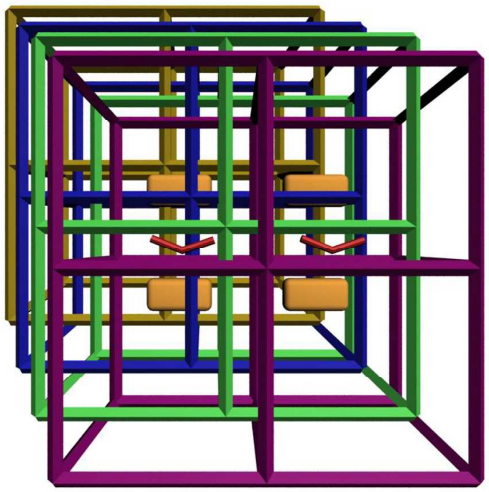

Fig. 4 A view down of the 4-fold interpenetrated motif containing water molecules and nitate anion in the channels.

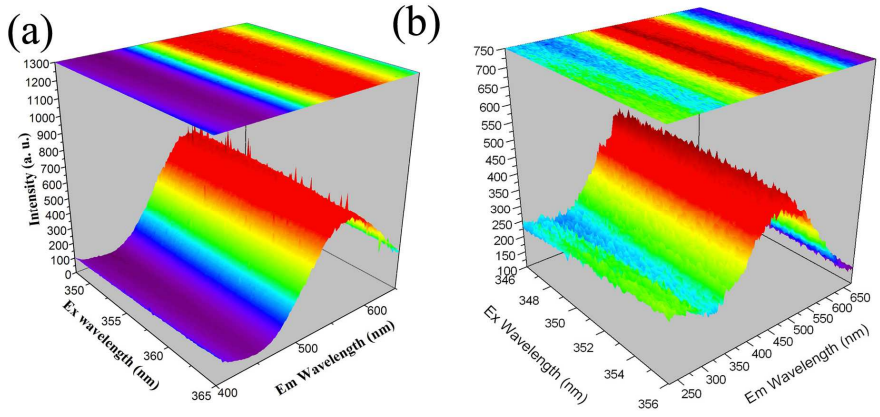

Fig.5 View of the luminescence spectrograms at room temperature for **1** and **1'**.

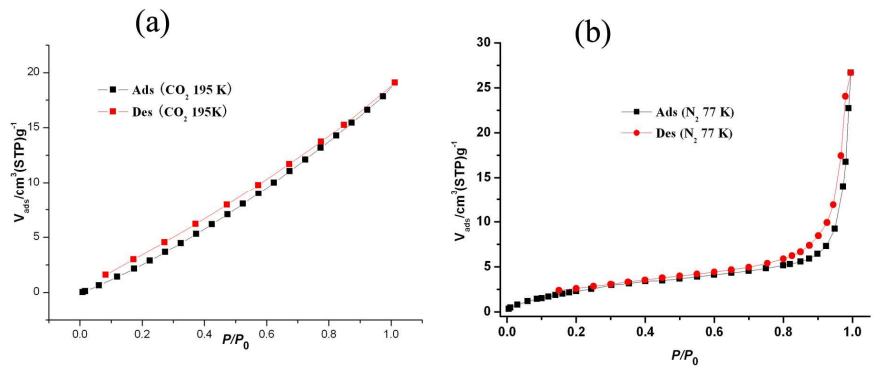

Fig. 6 (a) gas sorption isotherms at 195 K for CO_2 in **1**; (b) gas sorption isotherms at 77 K for N_2 in **1**

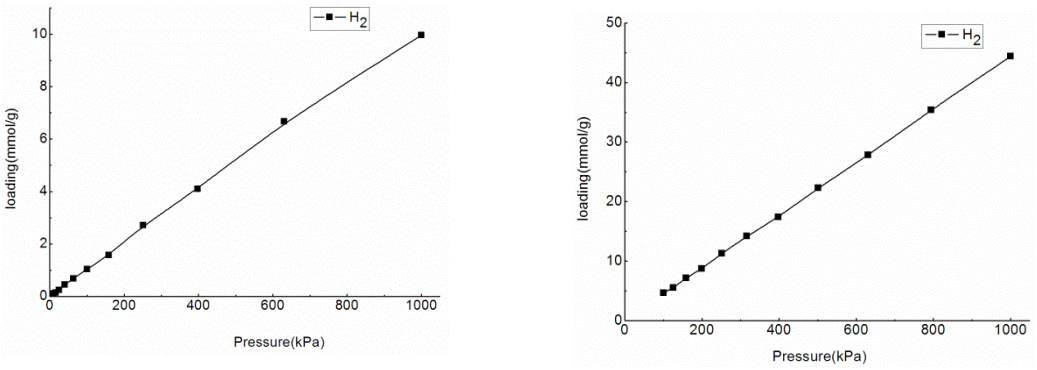

Fig. 7 Simulated adsorption isotherms of H_2 in MOF at 77 K with P = 0-1000 KPa in different environments of solvent molecules.

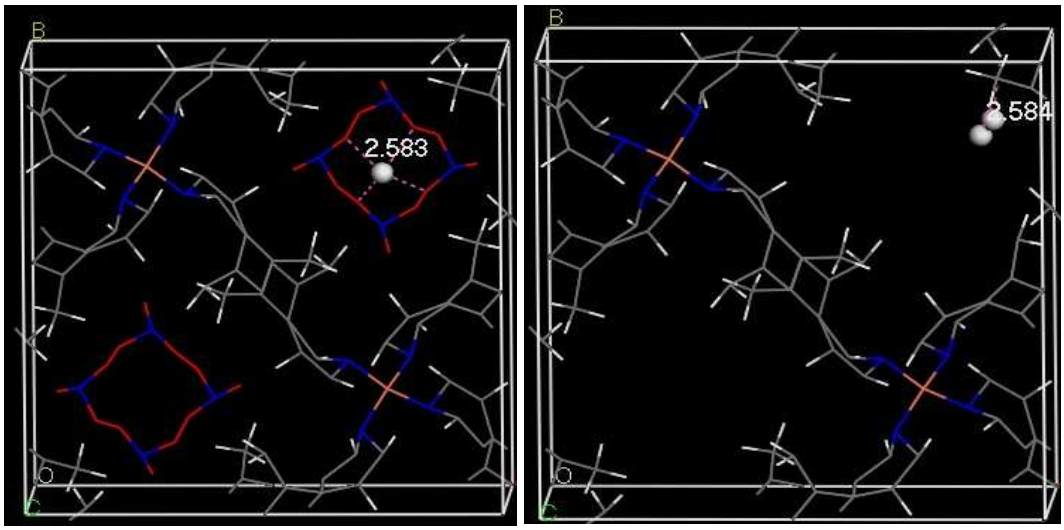

Fig. 8 Bonding sites between H_2 and MOF: (a) containing solvents (left), (b) without solvents (right).

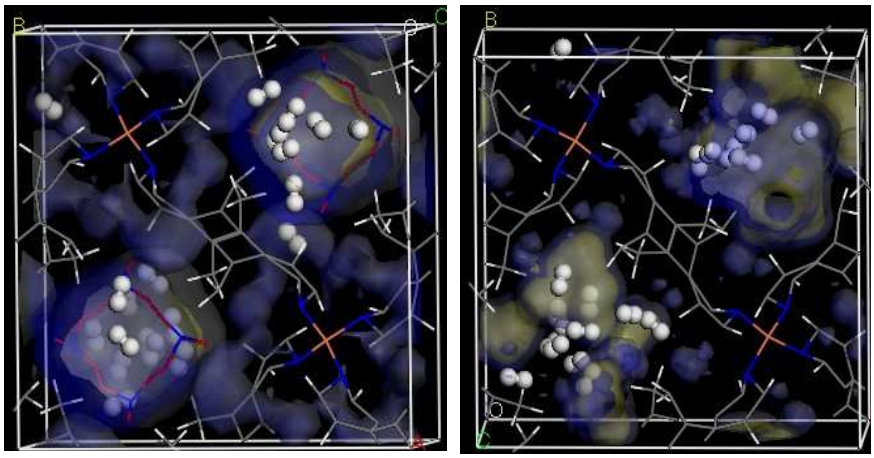

Fig. 9 Snapshots of MOF with H_2: (a) containing solvents (left), (b) without solvents (right).

Table 1 the crystallographic data of **1**.

Complex	**1**
Empirical formula	$C_{28}H_{40}CuN_5O_7$
Formula mass	622.19
Crystal system	tetragonal
Space group	*P 4/n*
a [Å]	16.417(2)
b [Å]	16.417(2)
c [Å]	6.598(2)
α [°]	90
β [°]	90
γ [°]	90
V [Å^3]	1778.3(6)
Z	2
d_{calcd} [g·cm^{-3}]	1.162
μ [mm^{-1}]	0.658
F(000)	656
Reflections/ unique	10804/2227
R(int)	0.0519
R_1,wR_2 [$I>2\sigma(I)$]	0.0482, 0.0823
R_1,wR_2 (all data)	0.1116, 0.0987

Table 2. Selected bond distances (Å) and angles (°) in **1-2**

1			
Cu1-N1#1	2.042(2)	N1-Cu1-N1#1	109.90(6)
Symmetric code: (i)	y-1/2, -x+1, -z+1		

A new 3D four-fold interpenetrated dia-like polymer: gas sorption and computational analyses

Jian Wu[a], Jian-Qiang Liu[b*], Zhen-Bin Jia[b], Qing-Lin Li[b], Kai-Bang Li[a], Hao Li[a], Carole Daiguebonne[c], Guillaume Calvez[c], Olivier Guillou[c*]

[a] *Guangxi Key Laboratory of Chemistry and Engineering of Forest Products, Guangxi University for Nationalities, College of Chemistry and Chemical Engineering, Nanning, Guangxi 530006, China*

[b] *School of Pharmacy, Guangdong Medical College, Dongguan 523808, China*

[c] *INSA, UMR 6226 "Institut des Sciences Chimiques de Rennes", F-35708 Rennes, France*

Corresponding author: jianqiangliu2010@126.com (J.-Q. Liu) and Olivier.Guillou@insa-rennes.fr(O. Guillou).

In this work, we present a four-fold interpenetrated 3D framework with a **dia**-like topology. The luminescent property of sample **1** and dehydrated sample **1'** was also explored.